Using Multi-Scale Spatial Data in Landslide Mornitoring and Landuse Classification Interpretation

Tienyin Chou[1], Chihheng Liu[2], Meilin Yeh[3], Yingchih Chen[4]

[1]Department of Land Management, GIS Research Center, Feng Chia University.
100 Wenhwa Rd., Taichung, Taiwan, R.O.C.
E-mail: jimmy@gis.tw
[2]Institute of Civil and Hydraulic Engineering, Feng Chia University
[3]GIS Research Center, Feng Chia University, Taichung, Taiwan
[4]GIS Research Center, Feng Chia University

Abstract

Owing to the rapid developments in the field of Geographic Information Systems and Remote Sensing techniques, various images sources have been widely available to identify ground changes information. Those commonly used multi-scale images provide the sources from macro to micro information and can be served as basic analysis platform in landslide monitoring and land use classification. Taiwan has a unique and vulnerable geological condition with potential disasters easily triggered by landslide occurrence due to typhoon and heavy precipitation each summer season. In order to identify and analyze those landslide information temporary and spatially, this research integrate satellite images, aerial survey data from aviation photography and LIDAR, and remotely controlled helicopter techniques to set up a diverse information network. Satellite images can fulfill the need for large area environmental inventory and land use classification. Digital Terrain Model generated by LIDAR and aerial photos can be used to mark the landslide area and estimate the size and volume. Remotely controlled helicopter can overcome the barriers of site accessibility and data transmitting simultaneously. This network then provides a less time and cost consuming platform by the idea of Grid methodology. The output from this research demonstrates the integration of heterogeneous data into a uniform communication interface to construct a thorough analysis mechanism. It is applicable and feasible to monitor the vegetation, terrain, and landscape changes through land use and land cover identification by multi-scale spatial data.

Keywords

RS, grid, multi-scale image, LIDAR, aerial photogrammetry

I. INTRODUCTION

Due to typhoon and torrential rains, SHI-MEN Reservoir watershed in Taiwan experienced serious landslide disaster with great sedimentation deposit along the river course. The government has started restoration and rebuilding tasks along the vulnerable areas and the final goal is to recover the natural environment.

In order to assist the government to achieve the goal of conservation, this research used remote sensing, Photogrammetry, LIDAR and Satellite Images to build multi-scale spatial information and integrated Grid mechanism to develop a uniform communication interface.

II. STUDY AREAS INTRODUCTION

SHI MEN watershed spans over an area of 75929ha divided into three major administrative boundaries of this area (as Figure 1). The size of this reservoir is the third in Taiwan region and embedded with various functions such as irrigation, electricity, water supply, flood control, ect. It is sensitive to landslide disaster due to steep slope, the rapid flow, unstable geology, typhoon and heavy rain (the serious disaster as shown in Table 1).
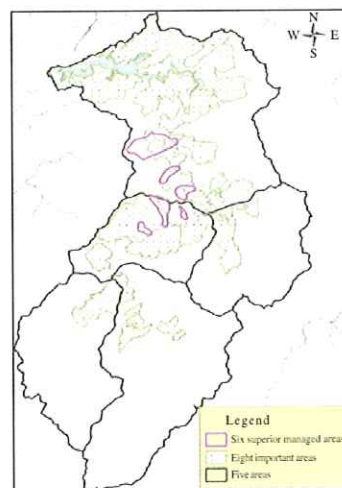

Figure 1. The three major administrative study area: Shi-Men Reservoir watershed

III. MATERIALS AND METHODS

This study used multi-scale remote sensing images and DEM data to analyze spatial environment of SHI-MEN watershed. The remote sensing images contain lots of information

Table 1. Serious disasters in Shi-Men Reservoir Historically

Year/Month	Typhoon	Average rainfall (mm)	Discharge (cms)	Increase Sludge ($10^4 m^3$)
1957/09	GLORIA	1375	10141	1947
1961/09	ELSIE	493	5703	503
1971/09	BESS	515	5172	523
1973/08	BETTY	607	5665	523
1976/08	BILLIE	454	5488	203
1985/08	NELSON	538	4906	370
1996/07	HERB	715	6363	867
2004/08	AERE	967	8594	2788
2005/08	MATSA	819	5322	1000

Data resource: GNorthern Region Water Resources Agency Ministry of Economic Affairs, National Science and Technology Center for Disaster Reduction.

Table 2. The comparison of Satellite image, Aerial photo, remotely piloted vehicle image

	SPOT 5	FORMOSAT-2	Quick Bird	Aerial photo	RPV image
Cost	Low	Low	The highest	Low	High
Contain range	Middle	Middle	Large	Small	The smaller
Spatial resolution	High	High	Higher	Higher	Higher
Temporal resolution	Fix	Fix	Fix	Depend	Depend
Mobility	Low	Low	Low	High	Higher
Stable	Depend on weather	Depend on weather	Depend on weather	Depend on weather	The weather affect is not important
Process	Easy	Easy	Easy	Hard	Hard
Small area application	Adaptive	More adaptive	Adaptive	More adaptive	Best adaptive

resources and the optimal choices are based on the final goal and budget limitation. Table 2 introduces the properties of different remote sensing images in Taiwan.

As a reference of comparison of Satellite image, Aerial photo, RPV image, and evaluation of the properties, advantages and disadvantages of various remote sensing images, this study adopted all feasible images to carry on research analyses. We collected, integrated and established vector data, raster data and study results from different aspects, such as change detection of landuse, investigation of disaster, the change analysis of water quality, conservation of reservoir, management of environmental ecology, sewage system, the implementation of management support system etc. On the other hand, according to Shi-Men Reservoir watershed past terrain data, we used LIDAR technology to get the updated high precision elevation data.

Therefore, in order to facilitate tasks of disaster monitoring, heterogeneous data must be integrated via a consistent communication interface. This research adopted the emerging grid technology to create a grid-based management mechanism. The core component of grid technology is to realize the exchange and share of resources through visualization, high-level abstraction, and combining heterogeneous data. Finally, we can provide much efficient information in managing the Shi Men Reservoir watershed through the grid-based

management mechanism. The total research flow chart is shown as Figure 2.

A. Using LIDAR technology to build the high precision DEM

The DEM of the study, 40M*40M area resolution was produced by photogrammetry in 1989. In time, the environment and the terrain have changed extremely. In order to understand the environmental changes of Shi Men Reservoir after a great deal of landslides, this study uses Airborne Laser Scanner ALS50(Table 3) producing by LEICA(Germany) to generate the high precision DEM(5m) data.

The system integrates GPS (Global Position System), IMU (Initial Measurement Unit), laser scanner, computer rack and Rollei Aerial Industrial Camera (Rollei AIC) to capture the elevation data and RGB images simultaneously and immediately. Besides the characteristics of high pulse rate (83kHz), wide field of view (75 degree), automatic adaptive roll compensation and max above ground level (4000 meters), this system also has a choreographed airborne platform and the calibration processes to enhance durability, convenient operation and scanning precision. In addition, the absolute coordinate of the plane is immediately located by GPS and is transformed to obtain the fire point. The transformation can be represented as a matrix (Eq.(1)). This means that t_x, t_y, t_z are the translations from GPS phase center to the fire point and
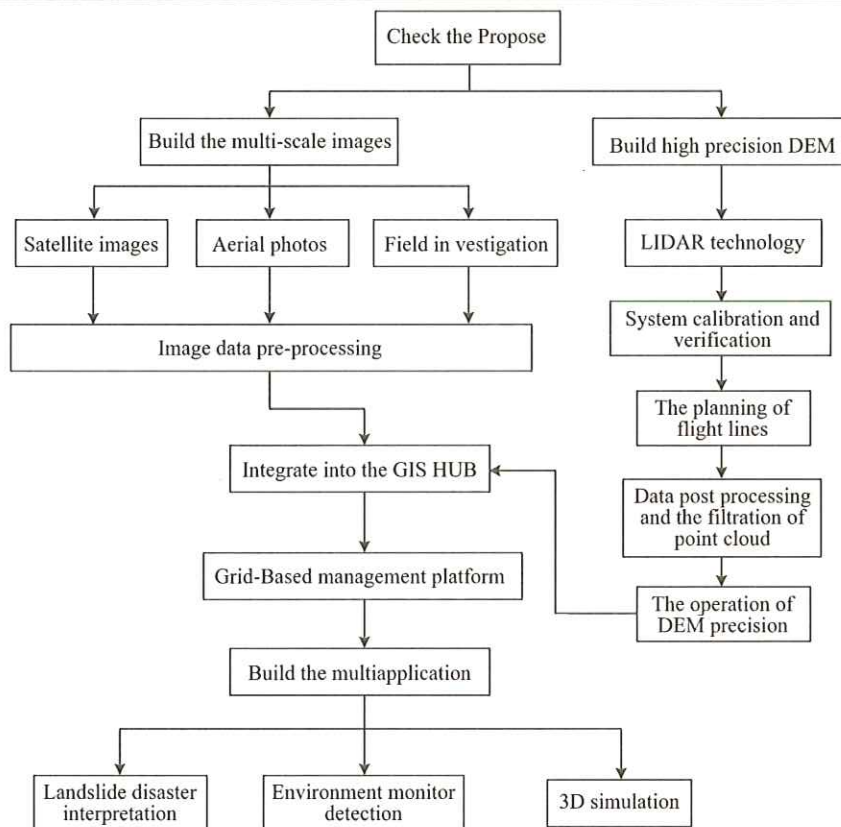
Figure 2. The Research flow chart

Table 3. ALS50 specification

| Itmes	Data/Operation
Scanning type	Oscillating,Mirror, Z-shaped
Pulse Rate	83kHz
Navelength	1064nm
Frequence	70Hz
Field of View	75 degree
Above ground level	200m——4000m
Adaptive roll compensation	Automatic
GPS/IMU	Novatel(2Hz)/ Applanix POS AV 510(200Hz)
ROLLEI AIC digital camera	4080×5440 pixels, 9μm/pixel 50mm metric lens
Scanner Size/Weight	37W×56L×24Hcm/30kg
Computer Size/Weight	48W×52L×64Hcm/64kg
Input Power	28V35Amps
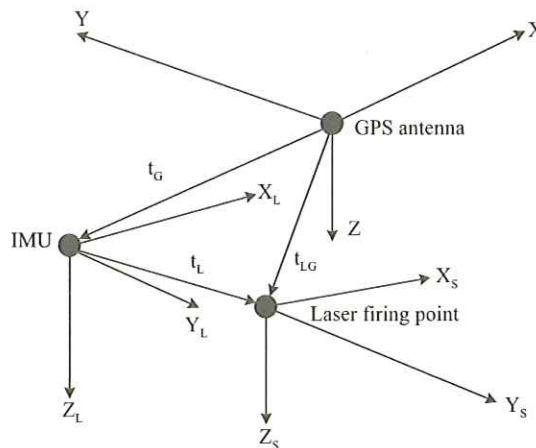
Figure 3. The coordinate system of airborne laser scanner

R_{IMU} is the rotation matrix which the coordinate system of the plane transforms to spatial coordinate system. The relationship between the coordinate systems is shown as Figure 3.

$$\begin{bmatrix} X_0 \\ Y_0 \\ Z_0 \end{bmatrix}_{\text{fire point}} = \begin{bmatrix} X \\ Y \\ Z \end{bmatrix}_{\text{GPS}} + R_{IMU} \times \begin{bmatrix} t_x \\ t_y \\ t_z \end{bmatrix}_{\text{tLG}} \qquad (1)$$

The producing processes of DEM include system calibration and verification, the planning of flight line in study area (there are 10 flight lines as shown in Figure 4) and the post-process of data operation and the filtration of the point clouds. Many scholars have raised the issue regarding the theory of strip adjustment. Concerning the elevation, Burman's observing function (eq. 2) has three unknown directions (dX,dY,dZ) and drifts (drift$_x$,drift$_y$,drift$_z$), and three axis angle offset (dr,dp,dh) and drifts (drift$_r$,drift$_p$,drift$_h$). The unknown parameter X is solved by the least square eq. 3. The observing matrix L is composed of ground points, houses and ground control points. P is the weight of each observation value.
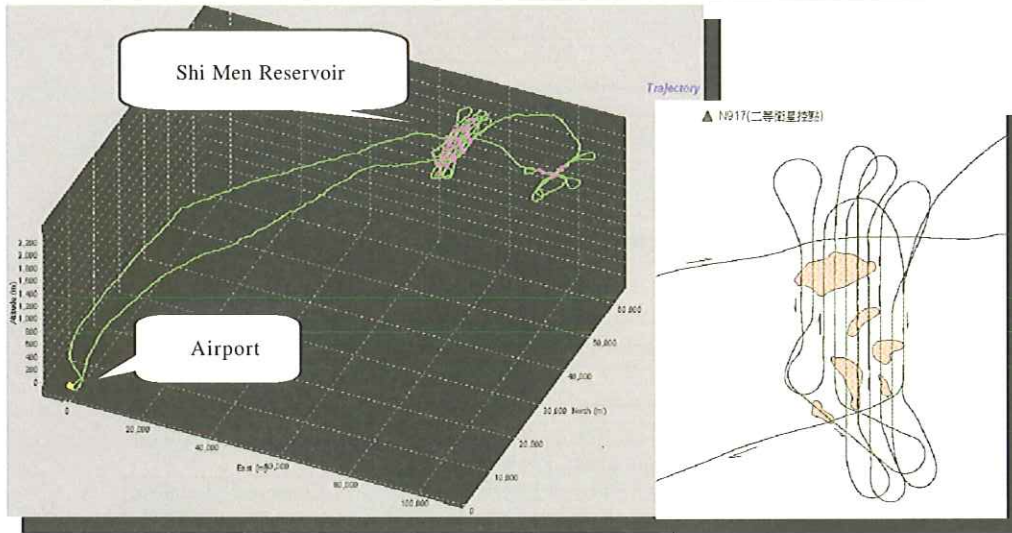
Figure 4. LIDAR flight line's orbit

$$Z_E - \hat{Z}_i = Z'_X \cdot (dX_d + t_1 \cdot drift_x) + Z'_Y \cdot (dY_d + t_1 \cdot drift_y) -$$

$$dZ_d + t_1 \cdot drift_z + \left(Z'_X \frac{\delta R_X}{\delta_r} + Z'_Y \frac{\delta R_Y}{+\delta_r} - \frac{\delta R_Z}{\delta_r} \right) \cdot \begin{pmatrix} l_X \\ l_Y \\ l_Z \end{pmatrix} \cdot$$

$$(dr + t_1 \cdot drift_r) + \left(Z'_X \frac{\delta R_X}{\delta_p} + Z'_Y \frac{\delta R_Y}{+\delta_p} - \frac{\delta R_Z}{\delta_p} \right) \cdot \begin{pmatrix} l_X \\ l_Y \\ l_Z \end{pmatrix} \cdot$$

$$(dr + t_1 \cdot drift_p) + \left(Z'_X \frac{\delta R_X}{\delta_h} + Z'_Y \frac{\delta R_Y}{+\delta_h} - \frac{\delta R_Z}{\delta_h} \right) \cdot \begin{pmatrix} l_X \\ l_Y \\ l_Z \end{pmatrix} \cdot$$

$$(dr + t_1 \cdot drift_h) + \tag{2}$$

$$AX = L + V; X = (A^T P A)^{-1} * A^T P L \tag{3}$$

After finishing the strip adjustment and verifying precision, the point clouds data is used to produce DSM and DEM. TerraScan software is used to classify, filter and thin the point data. TerraModeler software proceeds to produce the three dimensions surface model. Manual verification and editing is used to fix the errors in the surface model. Finally, the DEM and DSM in grid format are produced by the surface model. The whole operation flow chart is shown as Figure 5.

B. Grid

The idea of "GRID" is the solution to overcome the problems of heterogeneity, distribution and efficiency. Users can search and adopt information that is beneficial for the analysis and work through the process. All heterogeneous and distributed information is monitored and encrypted by the platform, all kinds of information can be exchanged according to the
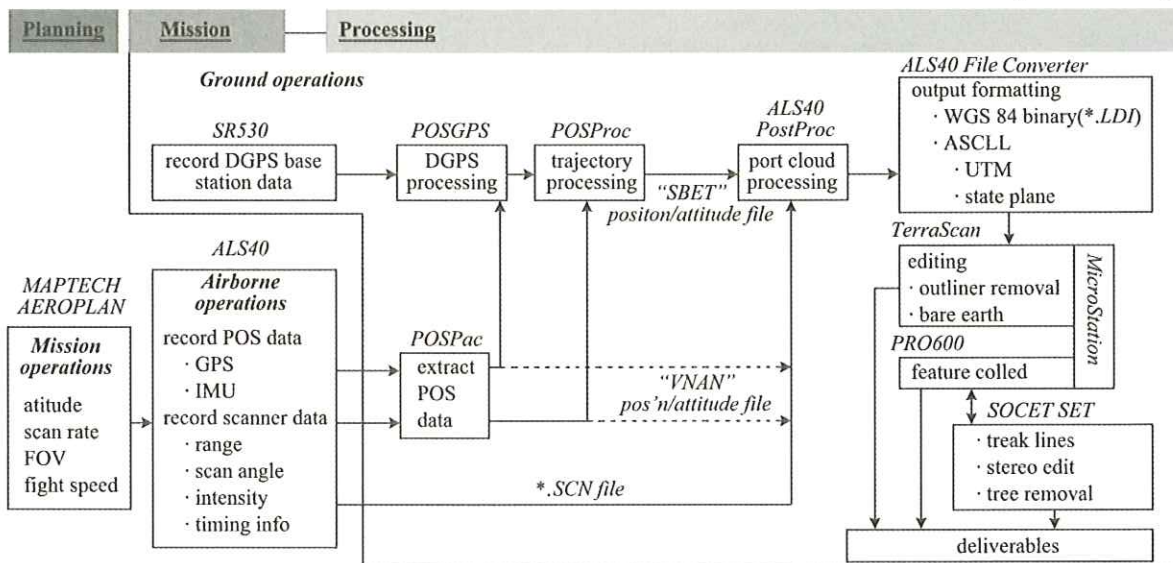

Figure 5. LIDAR operation flow chart

standard. As this framework is regardless of the original design of systems that locate into different departments, some different applications of "GRID" computing environment are developed internationally. "GRID" is a cluster of computing resources; it can combine all varieties of computing resources (all kinds of computers, network communications, storage equipments, data, extensibility, and adaptability, un-predictability of structure, autonomy and multiplicity of management) and develop a computing ability that is ubiquitous, reliable, standard and economically.

C. Remote sensing images interpretation

According to the aim of control, manage the district environment problem via remote sensing technology rapidly. The classification of spectral images is according to the solar reflection intensity of land surface which recoded by pixel of the image. By using appropriate mathematical and statistical algorithm, we calculated and analyzed the categories of land cover. The process makes an original satellite image transfer to a thematic layer with substantial geographic meaning (Lung-Shih Yang etc., 2000). The change detection of land use consists of three analytical parts: 1) land use interpretation using the RS images; 2) existing land use conditions; 3) environmental change analysis. The imagery processes are a series of procedures which include radiometric corrections, geometric corrections, enhancement, etc.

The supervised classification was applied to the satellite image. Existing map, aerial photographs and results of the field investigation were adopted during the classification process. In this way, it can ensure the high accuracy in classification of land use. Afterward, the accurate assessment is integrated with related GIS data, land use maps, historical data and ground true data from field surveying. The error matrix is employed in this research to estimate results of accuracy. The OA (Overall Accuracy), UA (User's Accuracy), PA (Producer's Accuracy) and KC (Kappa Coefficient) are four indexes to estimate the accurate analysis of the error matrix:

OA index is the number of correctly classified pixels and is calculated by the ratio of the sum of correctly classified pixels in all classes to the sum of the total number of pixels tested; PA indicates the number of correctly classified pixels in the sample points of ground truth reference data; terms as omission error; UA indicates the correctly classified rate. KC present the inaccuracy of the entirely image classification by the reciprocal operation within the error matrix, it also considers both of the factor of omission and commission (Cohen J., 1960), which is more acute indicator than UA, PA and OA .

The values ranges of Kappa is from 0 (no association, that is any agreement between the map and the ground truth equals chance agreement) through 1 (full association, there is perfect agreement between the two images) (Andrew K. Skidmore, 1999).

According to the pixel value, and spectrum reflection degree

of landuse, the spectrum characteristic in each band can be compared by categorized results to calculate Transformed Divergence (TD). After training site selection, TD was used to examine the training sample of divergent degree and overlapped situation to assess the selective sample data. The TD equations were shown as (4), (5).

$$TD_{ij} = 2000\left(1-\exp\left(\frac{-D_{ij}}{8}\right)\right) \qquad (4)$$

$$D_{ij} = \frac{1}{2}tr((C_i - C_j)(C_i^{-1} - C_j^{-1})) + \\ \frac{1}{2}tr((C_i^{-1} - C_j^{-1})(\mu_i - \mu_j)(\mu_i - \mu_j)^{\mathrm{T}}) \qquad (5)$$

Where

i, j: two classes, C_i: the covariance matrix of class i, μ_i: the average vector of class i, tr the trace of matrix - sum of the major diagonal

D. Environmental change analysis

Change detection is an imperative task due to different technologies (post-classification or pre-classification)often produce different maps of change (P.R. Coppin, 1991). The post-classification comparison approach is a change information extraction method, which is a "from-to" concept to obtain the transitional condition on the ground surface. The post-classification approach involves the analysis of differences between two independent categorization products. Application approaches include either visually imaged interpretation (pattern recognition), or computer data categorization (spectral analysis), or a combination of both (M.C. García-Aguirre, et al., 2005). It provides detailed information about the type of land cover/land use change for every pixel and/or polygon under examination (Jungho Im; John R. Jensen, 2005). Thus, post-classification was employed to compare the multi-temporal satellite images to process the change detection of land use in environment. Figure 6 (a) shows that it will cause an error of change monitoring while the same land class has the different categories. Figure 6 (b) shows that the different classified criterions classify different land classes into different categories. It is one of the fundamental problems of change monitoring. It is essential to completely comprehend the description of the classification when integrating the multi-temporal classification results. In order to minimize the proportion of error, uniform classified scheme and criterion are used.

IV. APPLICATION RESULTS

A. Discussion of landslide disaster interpretation

When a landslide occurs, it would cross and cover the original land cover, the spectral reflection would change the vegetation characteristic into non-vegetated characteristic. Comparing these images obtains and recognizes this information. The
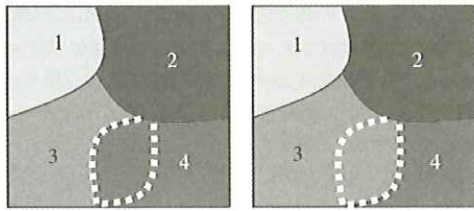
(a) The diagram of same land class number of two periods
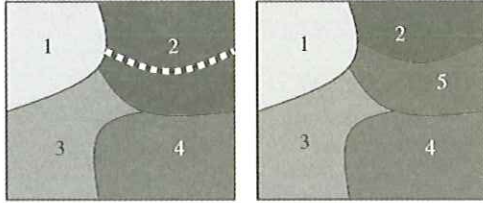
(b) The diagram of different land class number of two periods

Figure 6

Maximum Likelihood Classifier based on supervised classification and SPOT5 satellite image was employed to classify the large scale of land use types. The classified categories include forest, agriculture, landslide, water, lake, developed area and cloud. There are 173 training sites which have been chosen in 2006 SPOT5 satellite image. The TD index of each classified categories is higher than 1900, and the average is 1995.7. That shows the differential process effect is reasonable and it could assist the further image classification. The result is shown as Table 4. After image interpretation process, the overall accuracy is 91.25%. Secondly, in order to construct the detailed land use data, we used the aerial photographs and RTF to interpret near urban and populous area. The interpretation flow chart is shown as Figure 7. The related results are in Table 5 and Figure 8.

B. The discussion of environmental detection

Figure 9 presents the four-tier design of grid architecture. There are four layers each of which maps correspond to different grids: Data Layer, Middleware Layer, Business Logical Layer, and Presentation Layer. Layers of the grid structure are explained as follows.

The Data Layer includes unprocessed raw data which comes either from the estimated and detected by sensors, from files, or from web services. The Data Layer serves as the Sensor GRID in the grid project. The Middleware Layer functions as

Table 4. The TD index of training sits

	Water	Forest	Farm	Build up	bare	collapse	Road	Others
Water	0	2000	2000	2000	2000	2000	2000	2000
Forest	2000	0	1996.58	2000	2000	2000	2000	1973.26
Farm	2000	1996.58	0	1999.32	2000	1997.35	2000	1994.63
Build up	2000	2000	1999.32	0	2000	1990.72	2000	1995.28
bare	2000	2000	2000	2000	0	1975.44	2000	2000
collapse	2000	2000	1997.35	1990.72	1975.44	0	2000	1978.53
Road	2000	2000	2000	2000	2000	2000	0	2000
Others	2000	1973.26	1994.63	1995.28	2000	1978.53	2000	0

Table 5. The error matrix of satellite image classification

	Water	Forest	Farm	Build up	bare	collapse	Road	Others	Row sum	Ref. sum	Class. Number	Correct Number	PA	UA
Water	30	0	0	0	0	0	0	0	30	30	30	30	100%	100%
Forest	0	46	4	0	0	0	0	0	50	49	50	46	93.88%	92.00%
Farm	0	3	26	0	0	1	0	0	30	30	30	26	83.87%	86.67%
Build up	0	0	0	17	1	0	0	2	20	23	20	17	70.83%	85.00%
bare	0	0	0	1	25	4	0	0	30	33	30	26	78.79%	86.67%
collapse	0	0	0	3	6	185	2	4	200	193	200	185	95.85%	92.50%
Road	0	0	0	0	0	3	17	0	20	19	20	18	94.74%	90.00%
Others	0	0	0	2	1	0	0	17	20	23	20	17	73.91%	85.00%
Colum sum.	30	49	30	23	33	193	19	23	400	400	400	365		

OA=91.25%

Table 6. All kinds of interpretation results

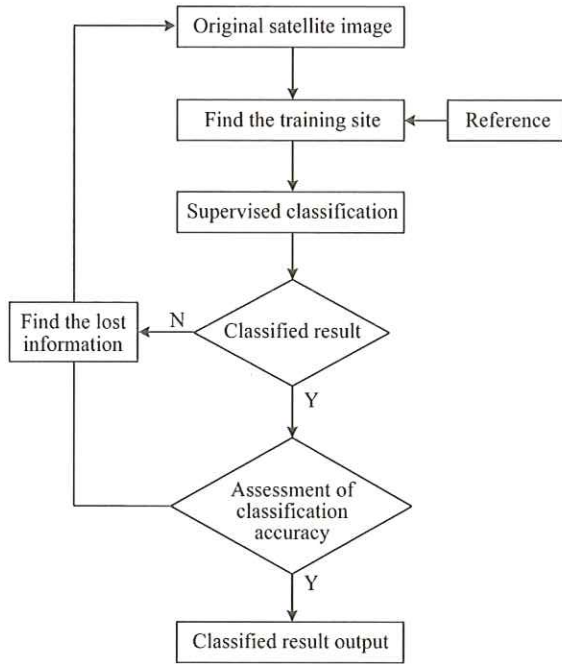| Class	Water	Woodlands	Farm	Building	Exposed	Collapse	Road	Others
Area(ha)	706.72	65690.1	1580.18	182.98	705.36	937.16	385.29	5816.62

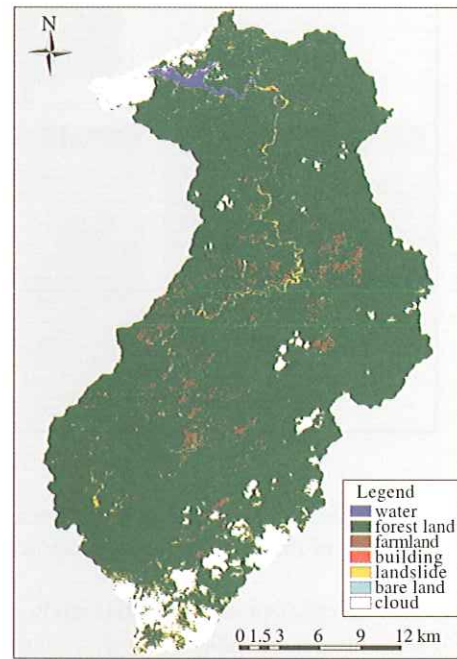**Figure 7.** Image interpretation Process

Figure 8. Results of classification Land cover in Shi-Men Reservoir watershed
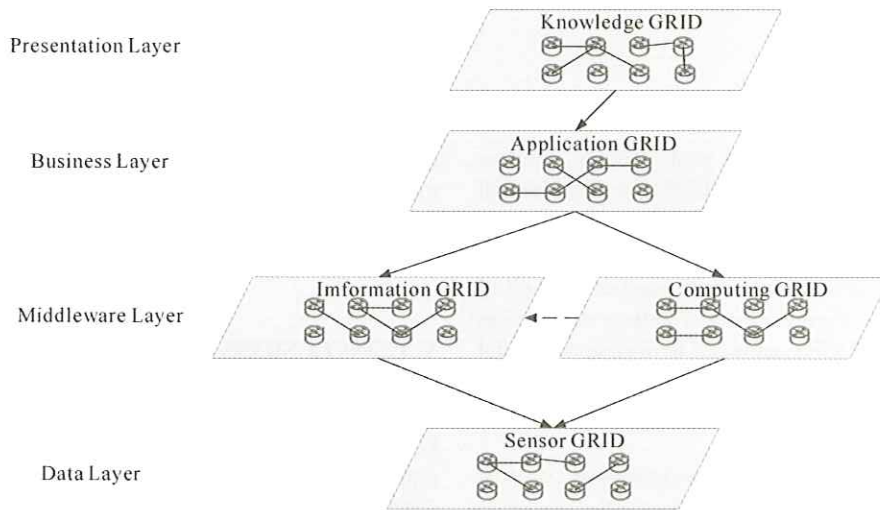

Figure 9. The four-tiers design of grid architecture

the middleware for high-level interface or services to access the Data Layer. It is responsible for converting the raw data into exchangeable data formats, Extensible Markup Language (XML) in this grid project and pre-processing the data by carrying out basic computations. For example, precipitation data is changed into the accumulated precipitation. The Middleware Layer covers the Information GRID and Computing GRID. The Business Layer accounts for integrating and adding values to heterogeneous computational patterns and processes of grid data. For instance, precipitation data is combined with the critical rainfall intensity for debris flow occurrence to predict potential debris flow torrents. The Presentation Layer displays the results of grid computation and integration. Association among information presented by

different grids and then grid wisdom are formed via continuous feedback and learning. The Presentation Layer can be mapped to the Knowledge GRID in the grid project.

As following the OGC consortium standard and infrastructure, the concepts of grid computing technology to integrate the type information of land cover, change detection information, water management technology and other database, are able to rapidly construct and enhance the capability of the data base. This research demonstrates the typical application of grid computing technology. The results were combined into the framework as 'business support system' as shown in Figure10. The GRID Application demonstrates the benefit of collaboration across organizations. In particular, the share of
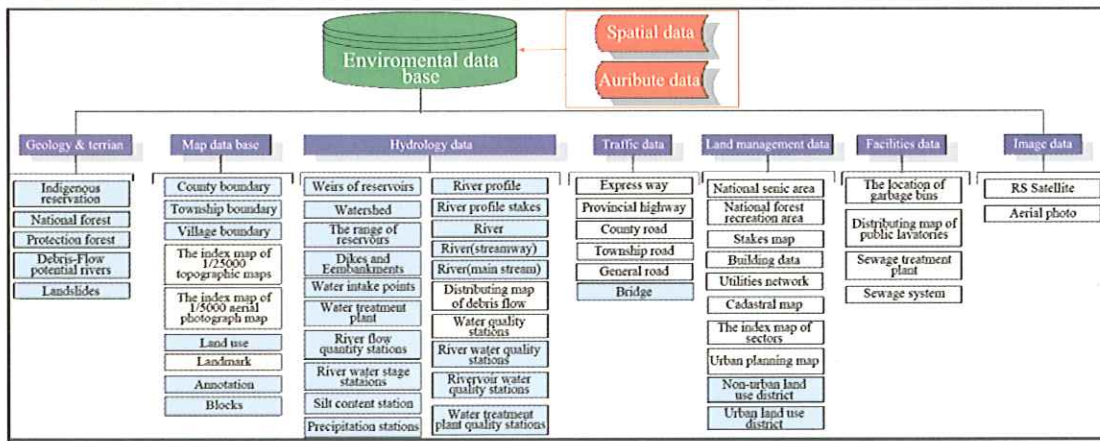
Figure 10. The framework of business support system

aerial photos, satellite images via the grid mechanism improves the interoperability of remote sensing application in Taiwan.

In order to provide efficient reference, this study collected or built multi-scale images, including the high resolution satellite image, high spatial resolution aerial photo and RPV image. As shown in Figure 11, there are three images of different scale, built by the data mentioned above. The engineering rebuild is closest to the original state.

C. 3D Simulations

LIDAR Aircraft-track parameter:
The raw data must be integrated in post-process, such as ground GPS basic-station, Aircraft-track GPS data, IMU Inertial navigation system, and search GPS refined-ephemeris data. POSPac software, and three dimensions coordinate and position of parameters, finds the optimum answer from all of the air-routes gradually. Figure 12 and 13 show calculation with track parameter by POSPac and GPS to resolve the orbital position in three-dimensional space precision analysis and integrate the IMU to calculate the accuracy orbital.

In order to work out the three dimension coordinate value of each echo and the intensity value under the coordinate system of WGS84, so-called the point cloud data, the post-processing software of ALS50 is used to process the LIDAR scanning data (recorded distance of the each, scanning angle, signal

intensity, and the each scanning echo and time), the parameters of the track of the airborne and the rate of the instrument. When we operate the point of cloud data, we should set the major parameters by software of ALS50 Post Processor. And then, involve the filtering processing of the ground point of cloud data, select the ground to classify of the TerraScan function, and also use TerraModel cloud editional function to cut a cross section by each 50m to discover the best ground trend line, and composes the 5M DEM file. Undergoing the ground points by artificial filtration processing may obtain Figure 14, the data of 5m DEM in whole area.

The 3D simulation result can display the surface details and reserving time, thus reducing the overall cost. This study integrated updated high resolution of aerial photos and high precision DEM data to simulate the 3D environment. The simulation result shows as Figure 15.

V. CONCLUSIONS

In this study, the concept of Grid is applied to integrate all kinds of environmental information in the watershed. The information shared portal has the benefit to monitor the sloping field and to analyze the changes of terrain comprehensively. The land cover data and terrain changes data are obtained by LiDAR and Remote Sensing technology. All the data proceeds to extract the land use and land cover information. This method

SOPT5 fusion image(2.5m)   Aerial photo(10cm)   RPV image

Figure 11. The three kinds of multi-scale images
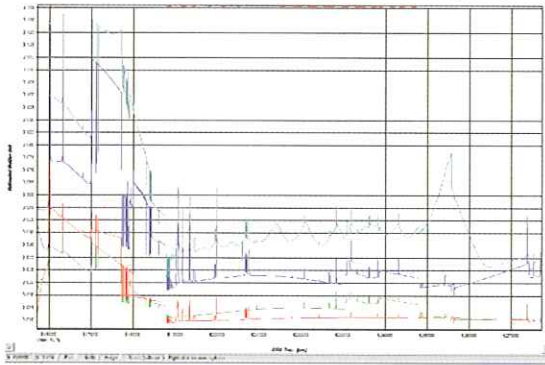
Figure 12. Using GPS to resolve the orbital position in three-dimensional space precision analysis (xy<2cm, z<4cm)
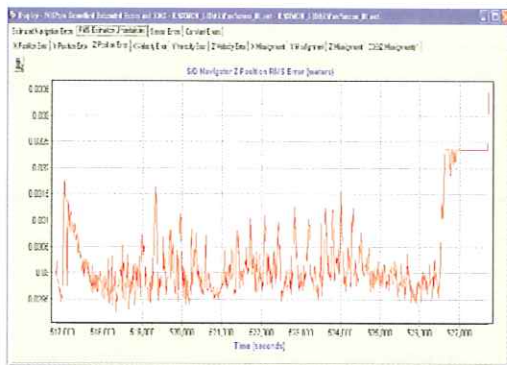

Figure 13. The accuracy of elevation after the accuracy orbital by using GPS+IMU (z<4cm)
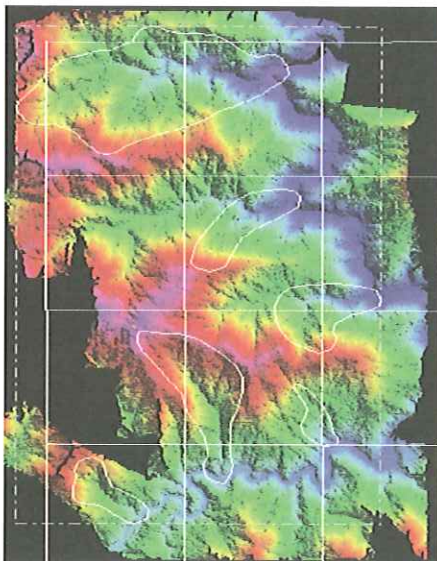

Figure 14. The data of 5m DEM in whole area

can monitor and manage well in land cover and land use from large-scale area to small-scale area. Regarding the terrain change, the point cloud of LIDAR is used to produce 5*5 DEM to analyze the terrain change after the data rectification and coordination. DEM does not only support the interpretation of remote sensing data but also convert plane data into three dimensions data. It means that the plane surface

before

after

Figure 15. 3D visualized change in Shi Men Reservoir watershed

change can be transformed into the change of the surface volume.

REFERENCES

[1] Andrew K. Skidmore, A. Stein, et al., 1999, Spatial Statistics for Remote Sensing, Kluwer Academic, pp.197—209.

[2] Cohen J., 1960, A coefficient of agreement for nominal scales, Educational & Psychological Measurement 20, pp.37—46.

[3] Jensen J R., 1986, Introductory digital image processing. N. J: Prentice-Hall. 397p.

[4] Jungho Im, John R. Jensen, 2005, A change detection model based on neighborhood correlation image analysis and decision tree classification, Remote Sensing of Environment 99, pp.326—340.

[5] Lung-Shih Yang, Tien-Yin Chou, 2000, Remote Sensing, Geographic Information Systems Research Center, Feng Chia University.

[6] Lillesand, Kiefer, 2000, Remote Sensing and Image Interpretation, 4th edition. New York: John Wiley and Sons. ISBN 0-471-25515-7.

[7] M C. García-Aguirre, R. Alvarez, R. Dirzo, A. Bernal, 2005, Post-classification digital change detection analysis of a temperate forest in the southwest basin of Mexico City, in a 16-year span, Analysis of Multi-Temporal Remote Sensing Images, 2005 International Workshop, pp.81—84.

[8] P R. Coppin, 1991, The change component in multitemporal Landsat TM images: Its potential for forest inventory and management. Ph. D. Thesis. University of Minnesota, EUA, 173p.